

Mineral Detection and Mapping Using Band Ratioing and Crosta Technique in Bwari Area Council, Abuja Nigeria.

Sadiya T. B., Ibrahim O., Asma T. F., Mamfe V., Nsofor C.J., Oyewmi A. S., Shar J.T., Sanusi M., Ozigis M.S.

Abstract- Landsat 7ETM+ of Bwari local government area of Abuja federal Capital Territory located in the middle belt of Nigeria was used to detect and map locations of hydrothermal alterations. Image processing methods used includes image rectification, spatial and spectral enhancement, band ratio, false colour composition (FCC) and Crosta technique. Band ratios $3/1$ and $(4/5 - 4/3)$ suggested the presence of ferric iron minerals and hydroxyl minerals respectively. Clay mineralization was detected using band ratio $5/7$. While false colour composite of bands $7:4:2$ was employed to delineate potential locations of hydrothermal alterations.

In both the band ratio and false colour composite there was interference from vegetation which affected the results. Subsequently, Principal Component Analysis (PCA) and Crosta technique were employed to suppress the interference. Resultant grey tone images from PCA shows white pixels depicting iron-oxide and hydroxyl mineral deposits. To enhance the location of mineral deposits, false colour composite of the resultant images and a sum of the two images were displayed as RGB respectively. Hydrothermal alteration zones hosting the mineral deposits were identified.

The identification of the hydrothermal alteration zones were correlated with the geological map and the ground-truth coordinates of already existing mines obtained from the study area.

Keywords- Band ratio, Colour Composite, Crosta technique, hydrothermal alteration zones, Mineral deposit, Principal Component Analysis, Remote sensing, and Landsat 7 ETM+.

1 Introduction

Nigeria is a country blessed with enormous mineral resources deposited all over the country [1]. Unfortunately, these mineral resources contribute only about 1% to the country's Gross Domestic Product (GDP) [2][3] due to government negligence of the mining sector and the proliferation of small scale illegal mining operations.

The small scale mining operations are carried out by untrained miners and the operations themselves are unregulated and without guidelines. This usually results in environmental degradation and loss of minerals [4]. Therefore, there is the need for a mineral resource inventory to aid the government in implementing better laws, regulations and mitigation to guide small scale miners in carrying out safer mining activities and also increase the country's GDP.

Considering that different types of mineral deposits are found all over the country, traditional method of mineral mapping can be costly and time consuming. A more modern method involves the use of remote sensing for the detection, identification and mapping of hydrothermally altered rocks which are a pointer to the locations of mineral deposits [5]. Remote sensing is the acquisition, processing and interpretation of images and related data which are acquired from airborne objects and satellites that record the interaction between object/phenomena and electromagnetic energy [6]. Remote sensing can detect and map hydrothermally altered mineral which lie on the earth's surface. Large areas of interests are mapped at a relatively fast pace while at the same time keeping the financial costs down [7]. Hydrothermal mineralization alteration is a process which alters the mineralogy and chemistry of the host rocks resulting in producing mineral assemblages

which vary according to the location, degree and duration of the alteration processes [7]. These minerals are unique in the way they absorb or reflect light along the electromagnetic spectrum due to their different chemical compositions, thus making it possible for minerals to be detected and mapped using remote sensing. Hydrothermally altered minerals (e.g kaolinite, allunite, muscovite etc.) are in most cases indications of a deposit of precious or economically viable mineral [8].

Several authors have analyzed and interpreted the remotely sensed hydrothermally altered mineral deposit data through band ratioing. For example Abdelsalam et al., in 2000 [9] used ETM+ band ratios (5/7, 4/5 and 3/1) in RGB to map the Beddaho alteration zone in northern Eritrea. [10] used Landsat ETM+ data for mapping gossans and iron rich zones exposed at Bahrah Area, Western Arabian Shield, Saudi Arabia. He found out that 4/5 ratio discriminate well between the gossans and iron-rich zones. Ratio 4/5 was also used to differentiate between the gossans, iron-rich rocks and surrounding rocks. The use of distinct spectral reflectance and absorption feature in ETM+ band ratio 5/7 and 3/1 highlights the presence of clay and iron minerals which is used to detect and map hydrothermal alteration zones by [6].

In Nigeria, there has been very little research in using remote sensing techniques to identify mineral deposits. One of the few carried out was [11] who applied band ratio technique and colour composite to map location of hydrothermal alteration within the Maru schist belt of Northwest Nigeria. In view of this, the aim of this paper is to detect and map the distribution of hydrothermally altered mineral deposit zones in the peri-urban area of Abuja as a means of initiating a mineral deposit inventory database for Nigeria.

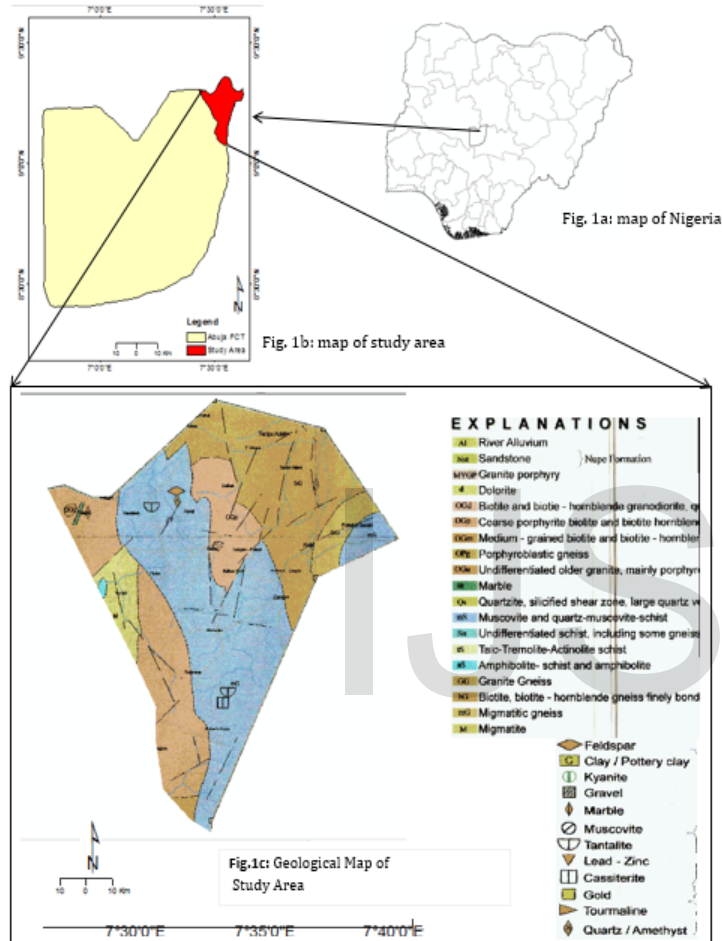
1.1 Geological Setting of Abuja

Nigeria lies within the zone of Pan-African reactivation (ca.550 Ma) to the east of the West African Craton, which has been stable since approximately 1600Ma. This mobile belt extends from Algeria across the Southern Sahara into Nigeria, Benin and Cameroon. Rocks of the Nigerian Basement Complex which is part of the Pan African Mobile Belt are intruded by Mesozoic ring complexes of Jos area and overlain unconformably by Cretaceous to Quaternary sediments forming the sedimentary basins. Three broad lithological groups have been distinguished in the Nigeria Basement Complex: A polymetamorphic, Migmatite-Gneiss Complex with ages ranging from Liberian (ca. 2800 Ma) to Pan-African (ca. 600Ma). The metavolcanosedimentary belt which is essentially made of the schists of low grade metasediments of greenschist facies of Proterozoic age (iii) the syntectonic to late tectonic granitoids of Precambrian to Lower Palaeozoic age which intrude both the gneiss complex and the schist belt [12][13][14][15][16].

The study area Abuja is predominantly underlain by the pre-Cambrian basement complex rocks. McCurry in 1976 [17] defined the basement complex of Nigeria as the reactivated ancient crystalline rocks which formed a suit of migmatite, gneiss and granite grouped as a single petrogenetic unit. Rahaman in 1988 [13] pointed out that the metamorphism of the basement rocks of Nigeria was polycyclic. Rahaman in 1976 [18] argued that about 60% of the basement complex rocks in north central Nigeria are made up of migmatite and gneissic rocks which have undergone at least three stages of deformational trends (metamorphism) before their present state. The local lithological units in the study area are migmatite-gneiss, granite, and schistose gneiss. Granite is the most wide spread rock unit occurring in several locations; they are

porphyritic and of medium-coarse-grained texture, Granites mostly occur as intrusive, low-lying outcrops around the gneiss. They are severely jointed and fairly incised by quartz veins with fractures trending northerly in the NNE-SSW, NNW-SSE directions.

1.2 Study Area and Geological Setting



2.0 Methodology

Throughout this study, two ground-truths exercises were carried out around the locations of past and present mining sites on 4th-July, 2014. It was found out that most of the mining sites are exploring granite for construction in economical quantities while other sites are precious minerals (e.g. tantalite, tourmaline, marble, quartz, etc.). Fig 6d shows image of a location where mining activity is currently going on.

2.1 Data Used and Pre-processing

Landsat 7 Enhanced Thematic Mapper Plus (ETM+) data scenes number 189/54(Path/Row) obtained on 1st-Jan-1998 when the weather was relatively dry was used. Geologic map of the study area was obtained from Nigerian Geological Survey [19] this will be use to compare locations of hydrothermal alteration zones detected with using remote sensing technique with locations of mineralization given in the geological map. The image was corrected for geometric distortions and projected to geographic (lat./long.) coordinate system and WGS-84 datum. The study area was subsetting from raster image (ETM+ data) using the shapefile of the Bwari LGA. The image was atmospherically corrected using Internal Average Relative Reflectance (IARR) method [20] and converted to surface reflectance.

2.2.0 Techniques Used

2.2.1 Band Ratio

Considering that each object has a unique spectral reflectance curve in each wavelength of the electromagnetic spectrum, band ratio can be used to emphasize the anomaly of target object by determining the band at which reflectance is high or point of highest absorption [21][22]. Band ratio also reduces the effect of topography, hence, enhancing the differences between spectral responses of each band [23]. Landsat ETM+ bands 3/1 can detect the

smallest amount of Ferric iron-bearing surfaces of hydrothermally altered rocks, sedimentary rocks, metamorphic rocks containing weathered, iron-bearing mafic minerals such as hornblende, biotite, sand deposits, and alluvium derived from such rocks will be identified with this index [24]. Clay mineralization is detected using the ratio 5/7 indicating that band 5 has reflectance in contrast to band 7 which has a high absorption. While subtracting band ratio 4/3 from 5/7 is done to remove the effect of vegetation interference in the detection of clay mineralization. Band ratio 5/4 is used in order to detect locations with hydroxyl mineralization, which is another indicator of hydrothermally altered zones [24][9].

2.2.2 Principal Component Analysis (PCA) and Crosta Technique

PCA is usually used for detecting and mapping the distribution of alteration in metallogenic provinces [21]. PCA is a multivariate statistical method that analyzes the Eigenvector loadings (eigenvalues) of a multispectral satellite image to determine the unique spectral response of different minerals and rocks contained in the image called Crosta Technique [5][7].

Sabins in 1996 [6] successfully adopted a methodology where PCA of Band sets 1347 and 1547 were run separately to determine the presence of iron-oxide and hydroxyl-rich minerals respectively. PC1 mapped albedo and topographic information while PC2 displayed the VIS/IR versus SWIR bands in contrasting signs [25].

The eigenvectors of PCs 3 & 4 were checked to see if they contain substantial loadings in opposite signs from input bands of 1 & 3 and 5 & 7, since these band pairs are expected to display contrasting response for iron and hydroxyl-rich minerals respectively [26].

3.0 Result and Analysis

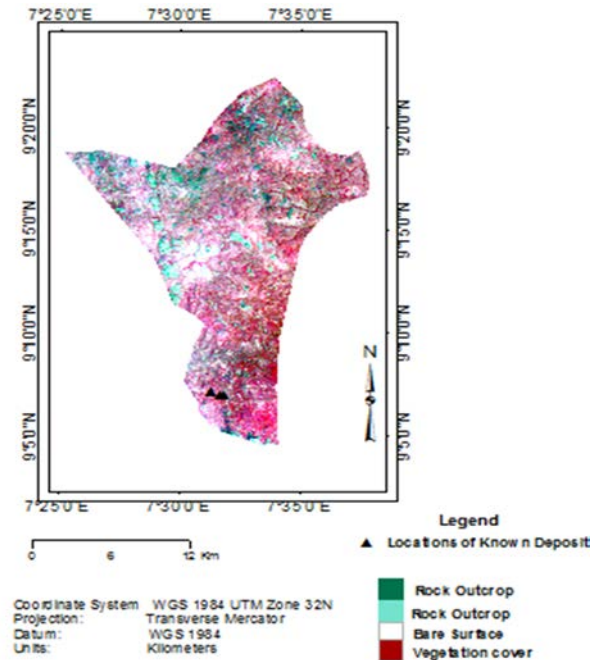


Fig 2: Bands 4:7:2 false colour composite of Landsat ETM+ subset in RGB showing study area in Bwari Area Council.

Using false colour composite, hydrothermal zones whose mineral spectral signatures are in near infrared (IR) to mid-infrared can be detected using ETM+ [27]. In Fig 2 altered minerals are seen in pale green, white and pale purple from creating a false colour composite of bands 4:7:2 in RGB respectively.

3.2.0 Band Ratios

Band ratio 3/1 highlighted areas in which any ferric iron mineral occurs pervasively or as coatings (Fig 3a). In Fig 3b band ratio (4/5 – 4/3) depicted hydroxyl mineral due to hydroxyl's high reflectance in band 4 and absorption minima in band 5. Subtraction of ratio 4/3 was carried out to reduce the effect of vegetation interference in the mineral detection. Clay mineralization was detected using the ratio 5/7. This shows that band 5 has reflectance in contrast to band 7 which has higher absorption property (see Fig 3c).

While ratio $(5/7 - 4/3)$ was used to subtract the effect of vegetation interference in the detection.

Due to spectral properties of the minerals, the colour composite of $(R-(3/1), G-((5/7)-(4/3))$ and $B-((4/5)-(4/3))$ was created to delineate the locations of hydrothermally altered rocks in pinkish to red and blue colours while vegetation appears green (Fig 4). To remove the effect of vegetation from interfering with mineral detection and mapping, statistical techniques called Principal Component Analysis (PCA) and Costa Technique were employed.



Fig 3a: Band ratio (3/1) Showing of Iron-Oxide mineralization in white

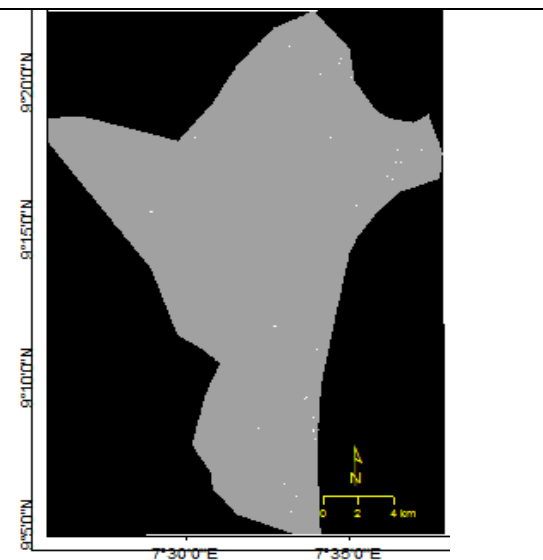


Fig 3b: Band ratio $((5/7)-(4/3))$

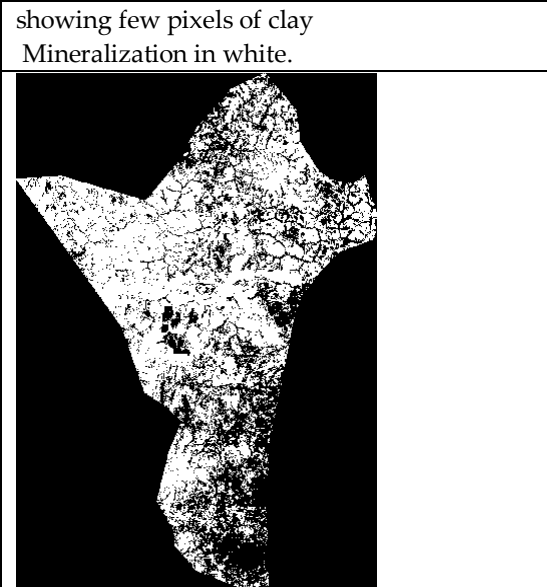


Fig 3c: Band Ratio $((4/5)-(4/3))$ showing Hydroxyl mineralization in white pixels.

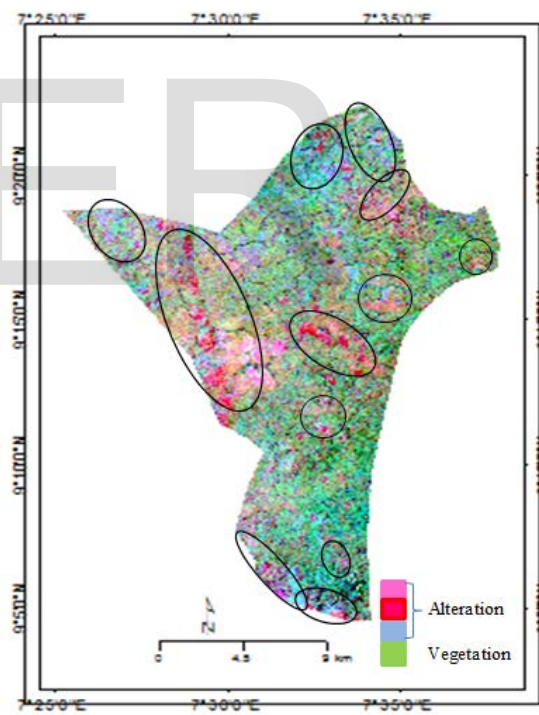


Fig 4: colour composite of $(R-(3/1), G-((5/7)-(4/3))$ and $B-((4/5)-(4/3))$ hydrothermally altered rocks in pinkish to red and blue colours while vegetation is in green.

3.3.0 Principal Component Analysis and Crosta Technique

The Principal Component Analysis was performed on two sets of band combination; 1457 and 1347. The PCA eigenvector values are shown in Tables 1 & 2. In Table 1, PC4 appears to have mapped iron-oxide minerals in dark pixels as observed in Band 3 which has high eigenvector value of -0.901413. So also in Table 2, PC4 appears to have mapped hydroxyl minerals in dark pixels. This is observed in Band 5 having a higher eigenvector value (-0.580019) compared to PC3 eigenvector value (-0.337910) in the same Band.

To display the iron-oxide and hydroxyl minerals in bright pixels, the negative of each image was taken (Figs 5a & 5b). In the resulting image bright pigmentation (Fig 5a) was due to the high reflectance of iron-oxide in band 3 and absorption minima in band 1; this image is called F-image. The bright pixels of hydroxyl mineral (Fig 5b) was due to the high reflectance in band 5 and absorption in band 7 [24][25]; this image is called H-image.

Eigenvector	Band 1	Band 3	Band 4	Band 7
PC 1	0.445965	0.381777	0.712609	0.384122
PC 2	0.177587	-0.142172	0.434724	-0.871358
PC 3	-0.826092	-0.146589	0.530668	0.120308
PC 4	0.295211	-0.901413	0.146950	0.280555

Table1: Principal component analysis of bands 1347 for Fe-oxides mineral

Eigenvalues	Band 1	Band 4	Band 5	Band 7
PC 1	0.382319	0.610790	0.607731	0.333812
PC 2	0.297129	0.579880	-0.424331	-0.628806
PC 3	0.823226	-0.343280	-0.337910	0.300457
PC 4	-0.296388	0.415733	-0.580019	0.634742

Table2: Principal component analysis of bands 1457 for hydroxyl minerals

False colour composite of the images corresponding to F-image, H-image and the sum of both (i.e. F-image + H-image) are displayed as RGB composite (i.e. F-image (R), H-image (G), F+H (B)) to allow the identification of

hydrothermally altered rocks (Fig. 5) in pinkish to red colour.

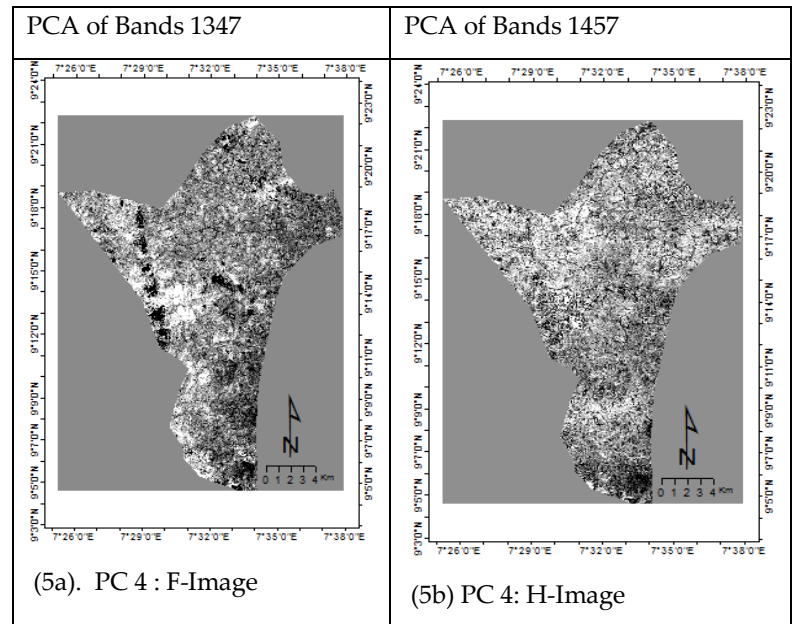


Fig 5a & 5b: Showing Iron-oxide and hydroxyl minerals in white pixels.

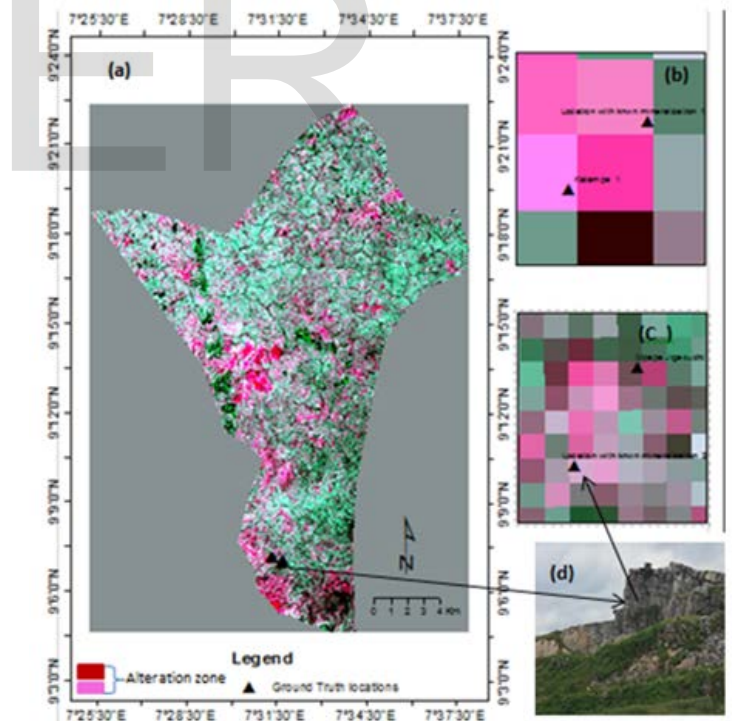


Fig 6: Colour composite of R(F-image), G(H-image) and the sum of B-(F+H). (b) Shows pixels of ground-truth site 1&2. (c) Represent pixels of ground-truth sites 3&4. (d) Image of one of Katampe quarry sites.

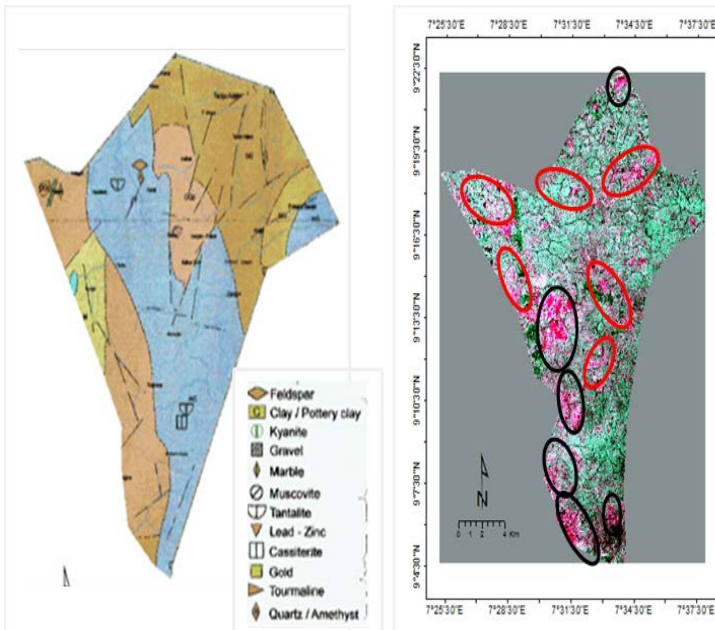


Fig 7: comparing remote sensing data with existing geological map on location of mineral deposits. Red polygons indicate locations corresponding to known locations on geological map while black polygons represent newly detected sites.

4.0 Discussion

False colour composite, band ratios and principal component analysis were utilized in order to spectrally enhance the response of different minerals such as iron-oxide, clay and hydroxyl which represent hydrothermal alteration zones such as the ones in Katampe (Fig 6d). From principal component analysis; in both tables PC1 have positive eigenvalue loadings which makes material identification using spectral signature impossible [27]. However, PC4 (Fig 5a) contains the spectral information depicting the iron-oxide bearing minerals in the study area which is much more than the amount detected using band ratio of 3/1. This is because PCA excludes the effect of vegetation signature interference [28]. It can be seen that the iron-oxide concentrations formed little clusters, occurring mostly in the northwest, north-central and eastern portions of the image. These areas coincide with

locations being mined for granite, tantalite, marble and other precious stones (as observed during the ground verification exercise) and also with the geological map (red polygons in Fig 7). So also from Fig 7 the black polygons represent other detected potentially interesting sites that are absent in the geological map. These sites are subject to further investigation.

Both the PC4 (Fig 5b) and band ratio (Fig 3c) indicate a large concentration of hydroxyl bearing minerals probably due to sericitisation during the alteration process, with the highest concentration in the north-northwest and north-east. This explains why there are few pixels of clay mineralization; this is because concentration of clay mineralization varies with the concentration of hydroxyl mineral [29]. Even though the band ratio colour composite (i.e. RGB) highlighted the spatial distribution of mineralized surfaces (Fig 4), it still exaggerated the extent of mineralization by depicting un-mineralized rock-outcrop and/or bare surface as hydrothermal alteration zones. This might be due to the effect of vegetation interference and other lithologies having same spectral signatures with the actual mineral deposits.

Fig 7 reveals corresponding mineral deposits location on satellite image and those observed on the geological map. Hydrothermal deposits are products of hydrothermal processes. These deposits form economic reserves when they are concentrated in veins, and other voids. Veins and lodes consist of the infillings of fissures and fractures developed in the outer part of an intrusive body or in the surrounding roof and wall-rocks. Veins which contain metalliferous minerals are termed lodes [30]. Minerals such as quartz, pyrite, topaz, and tourmaline are commonly associated with metalliferous minerals in lodes. Just as obtained from the geology of the study area, metals which

are commonly associated in this way with acid rocks include copper, lead, zinc, arsenic, tungsten, gold and silver. In the study area, tin exists in the form of cassiterite (SnO_2), tantalite $[(\text{Fe},\text{Mn})\text{Ta}_2\text{O}_6]$, the primary source of tantalum is presently being mined. Quartz in granites and gravels are majorly being mined for construction purposes while marble and tourmaline are being mined in small quantities by artisans.

5.0 Conclusion

Application of Crosta's Technique with two sets of four spectral bands (i.e. tables 1 & 2) has proven to be more efficient for the mapping of hydrothermal alteration zones in the form of iron-oxide and hydroxyl minerals. This can be seen in Fig.6 where locations of mineralization are represented in pinkish to red colouration.

This study has established that the combined use of spatial and spectral resolution of satellite data could result in the detection and mapping of locations with known and unknown mineral deposit. Intrusion-related mineralization indicators such as iron-oxide, clay and hydroxyl minerals in the Bwari local government area mining locations have been detected using Landsat7 ETM+ dataset and the technique used in this investigation. The techniques used allowed the removal of spectral effect of vegetation from the EMT+ images resulting in the detection of the mineral deposit. This research could be made better by using hyperspectral images to determine the exact indicator mineral deposit in the study area.

References

- [1] O. Uzoka, "Chairman, House Committee on Solid Minerals, National Assembly, Nigeria", Interview with Thisday Newspapers, available from

- : <http://www.thisdayonline.com/archive/2001/08/26/200110826news12.html>, (March 17, 2002).
- [2] L. Awute "Permanent Secretary, Ministry of mines and steel Development, Nigeria". Interview with Vanguard newspaper at the Nigerian-Brazil Investment forum in Abuja. Vanguard Newspaper, (2013). Available from: <http://www.vanguardngr.com/2013/02/nigeria-loses-n8trn-to-illegal-gold-mining/>. (june 29, 2014)
- [3] Nigeria: Mining – Overview, 2014. Available from: <http://www.mbendi.co.za/indy/ming/af/ng/p0005.htm>, (20 April, 2014)
- [4] I. Aigbedion, & S.E. Iyayi, "Environmental effect of mineral exploitation in Nigeria". *International Journal of Physical Sciences*, 2 (2), 033-038, 2007.
- [5] A.P. Croster, C.R.S. Filho, F. Azevedo & C. Brodie, "Targeting key alteration minerals in epithermal deposits in Patagonia, Argentina, using ASTER imagery and principal component analysis". *INT. J. Remote Sensing*, 24(21), 4233–4240, 2003.
- [6] Sabins, F.F. "Principles and Interpretation" in W.H. Freeman (3rd ed.), *Remote Sensing* (New York NY: 494), 1997.
- [7] M.B. Mia & Y. Fujimitsu "Mapping hydrothermal altered mineral deposits using Landsat 7 ETM+ image in and around Kujū volcano, Kyushu, Japan", *Journal of Earth System Science*, 121(4), 1049–1057, 2012.
- [8] J. B. Torre, J. G. R. Ayuga, J. Bonatti, M. M. Sacristán & R.M. Marín "Detection of hydrothermal alteration using a principal component analysis applied to hyperspectral map data on the Turrialba Volcano, Costa Rica", *International Archives of the Photogrammetry, Remote Sensing and Spatial Information Sciences*, XXXIX-B7, 2012.
- [9] M.G. Abdelsalam, R.J. Stern, & W.G. Berhane "Mapping gossans in arid regions with Landsat TM and SIR-C images: the Beddaho Alteration Zone in northern Eritrea", *International Journal of African Earth Science*, 30(4), 903-916, 2000.
- [10] A. Madani "Utilization of landsat etm + data for mapping gossans and iron rich zones exposed at Bahrah Area , Western Arabian Shield , Saudi Arabia", 35-49, 2009.
- [11] E. A. Kudamnya, W.T. Andongwa, & J.O. Osumaje, "Hydrothermal Mapping of Maru Schist Belt, North-Western Nigeria Using Remote sensing Technique". *International journal of civil engineering*, 3(1), 59-69, 2014.
- [12] K.C. Burke & F.J. Dewey. Orogeny in Africa. In: Dessauvagie, T.F.J. and Whiteman, A.J. (Ed.), *African Geology*, (Ibadan University Press, Ibadan) 583-608, 1972.
- [13] M.A. Rahaman, "Recent advances in the study of basement complex of Nigeria". In *Precambrian Geology of Nigeria, Nigeria Geological Survey*, , 11–43, 1988.
- [14] E. Annor, & S.Freeth," Thermo-tectonic evolution of the basement complex around Okene, Nigeria, with special reference to deformation mechanism, Precambrian Research" , 28:269-281, 1985.
- [15] I. Odeyemi,"Lithostratigraphy and structural relationships of the upper Precambrian metasediments in Igarra area, southwestern Nigeria, Precambrian Geology of Nigeria", *Nigeria Geological Survey*, 111–125, 1988.

- [16] E. Annor, "A note on the geology of the Isanlu area, in the Egbe-Isanlu schist belt, S.W. Nigeria", *Journal of Mining and Geology*, 47-52, 1995.
- [17] P. McCurry, "The Geology of the Precambrian to lower Paleozoic rocks of northern Nigeria", In K. C. (ed.), *A review In: Geology of Nigeria*, (Lagos, Nigeria: Elizabethan Publishing Co), 15-29, 1976.
- [18] C. Ajibade, "Proterozoic crustal development in the Pan african regime of Nigeria" C. A. (Ed.), *Geology of Nigeria*. Lagos, (Elizabethan Publishing Co), 57-69, 1989.
- [19] Nigeria Geological Survey, 2014.
Available: <http://wrf.nigeriagovernance.org/organizations/view/870>, (March 16, 2014)
- [20] F.A. Kruse, G.L. Raines, & K. Watson. Analytical techniques for extracting geologic information from multichannel airborne spectroradiometer and airborne imaging spectrometer data. In *Int. Symp. on Remote Sensing of Environment 4th Thematic Conference on Remote Sensing for Exploration Geology*, Ann Arbor, Michigan, *ERIM*, 1-4 April, 309-324, 1985.
- [21] R. Nouri, M.R. Jafari, M. Arain, & F. Feizi, Hydrothermal Alteration Zones Identification Based on Remote Sensing Data in the Mahin Area, West of Qazvin Province, Iran, *World Academy of Science, Engineering and Technology*, V6, 2012.
- [22] T. San, E. O. Sumer, & B. Gurcay, "Comparison of band ratioing and spectral indices methods for detecting alunite and kailinite minerals using ASTER data in Biga region, Turkey, Geo-Imagery Bridging Continents" XXth *ISPRS Congress*, Istanbul, Turkey, July 2004.
- [23] A. Ghulam, R. Amer, & T. M. Kusky, "Mineral Exploration and Alteration Zone Mapping in Eastern Desert of Egypt using Aster Data", *ASPRS Annual Conference San Diego*, California, 2010.
- [24] B.W. Rockwell, "Automated mapping of mineral groups and green vegetation from Landsat Thematic Mapper imagery with an example from the San Juan Mountains Colorado: U.S. Geological Survey Scientific Investigations *http://pubs.usgs.gov/sim/3252/*, 2010.
- [25] N. A. Kenea, & H. Haenisch, "Principal component analysis for lithologic mapping and alteration mapping: Examples from the Red Sea Hills". *International achievements of photogrammetry and remote sensing*. XXXI, part B7, 1996.
- [26] W. P. Loughlin, "Principal component analyses for alteration mapping", *Photogrammetric Engineering and Remote Sensing*, 57 (9), 163-1169, 1991.
- [27] J.R. Jensen, "Introductory Digital Image Processing". (Pearson Prentice Hall: Upper Saddle River), 2005.
- [28] A.P., Crosta, & J.M.M. Moore, "Enhancement of Landsat Thematic Mapper imagery for residual soil mapping in SW Minas Gerais State, Brazil: a prospecting case history in Greenstone belt terrain", *Proceedings of the 7th ERIM Thematic Conf.: Remote Sensing for Exploration Geology*, 1173-1187, 1989.
- [29] B., Pour, M., Hashim, & J. B. Genderen, "Detection of hydrothermal alteration zones in a tropical region using satellite remote sensing data: Bau goldfield, Sarawak, Malaysia", *Ore Geology Reviews* 54:181-196, 2013.
- [30] Blyth, F.G.H., & De Freitas, M.H. (1984). *Geology for Engineers* (7th ed), (Edward Arnold (Publishers) Ltd, London).